



HAL
open science

Measurement of the semileptonic CP asymmetry in $B^0 - \bar{B}^0$ mixing

R. Aaij, B. Adeva, M. Adinolfi, A. Affolder, Ziad Zj Ajaltouni, S. Akar, J. Albrecht, F. Alessio, M. Alexander, S. Ali, et al.

► **To cite this version:**

R. Aaij, B. Adeva, M. Adinolfi, A. Affolder, Ziad Zj Ajaltouni, et al.. Measurement of the semileptonic CP asymmetry in $B^0 - \bar{B}^0$ mixing. *Physical Review Letters*, 2015, 114 (4), pp.041601. 10.1103/PhysRevLett.114.041601 . in2p3-01070321

HAL Id: in2p3-01070321

<https://hal.in2p3.fr/in2p3-01070321>

Submitted on 20 Sep 2023

HAL is a multi-disciplinary open access archive for the deposit and dissemination of scientific research documents, whether they are published or not. The documents may come from teaching and research institutions in France or abroad, or from public or private research centers.

L'archive ouverte pluridisciplinaire **HAL**, est destinée au dépôt et à la diffusion de documents scientifiques de niveau recherche, publiés ou non, émanant des établissements d'enseignement et de recherche français ou étrangers, des laboratoires publics ou privés.



Measurement of the semileptonic CP asymmetry in $B^0-\bar{B}^0$ mixing

The LHCb collaboration[†]

Abstract

The semileptonic CP asymmetry in $B^0-\bar{B}^0$ mixing, a_{sl}^d , is measured in proton–proton collision data, corresponding to an integrated luminosity of 3.0 fb^{-1} , recorded by the LHCb experiment. Semileptonic B^0 decays are reconstructed in the inclusive final states $D^-\mu^+$ and $D^{*-}\mu^+$, where the D^- meson decays into the $K^+\pi^-\pi^-$ final state, and the D^{*-} meson into the $\bar{D}^0(\rightarrow K^+\pi^-)\pi^-$ final state. The asymmetry between the numbers of $D^{(*)-}\mu^+$ and $D^{(*)+}\mu^-$ decays is measured as a function of the decay time of the B^0 mesons. The CP asymmetry is measured to be $a_{\text{sl}}^d = (-0.02 \pm 0.19 \pm 0.30)\%$, where the first uncertainty is statistical and the second systematic. This is the most precise measurement of a_{sl}^d to date and is consistent with the prediction from the Standard Model.

Published in Phys. Rev. Lett.

© CERN on behalf of the LHCb collaboration, license CC-BY-4.0.

[†]Authors are listed at the end of this Letter.

The inclusive charge asymmetry measured by the D0 collaboration in events with same charge dimuons [1] shows one of the largest discrepancies with the Standard Model and it may be a first hint of physics beyond our current understanding (e.g., Refs. [2–4]). This asymmetry is sensitive to CP violation in the mixing of neutral B mesons. The neutral B^0 meson and its antiparticle \bar{B}^0 are flavour eigenstates, formed from a mixture of two mass eigenstates. The time evolution of this two-state system results in flavour-changing $B^0 \rightarrow \bar{B}^0$ and $\bar{B}^0 \rightarrow B^0$ transitions. Violation of charge-parity (CP) symmetry may occur due to this process if the probability for a B^0 meson to transform into a \bar{B}^0 meson is different from the reverse process. When a meson produced in the B^0 eigenstate decays semileptonically to a final state f , the charge of the lepton reveals the meson flavour at the time of decay. In such decays, “wrong-sign” transitions, like $B^0 \rightarrow \bar{f}$, can only happen due to the transition $B^0 \rightarrow \bar{B}^0 \rightarrow \bar{f}$. The flavour-specific (semileptonic) asymmetry is defined in terms of partial decay rates Γ as

$$a_{\text{sl}}^d \equiv \frac{\Gamma(\bar{B}^0 \rightarrow f) - \Gamma(B^0 \rightarrow \bar{f})}{\Gamma(\bar{B}^0 \rightarrow f) + \Gamma(B^0 \rightarrow \bar{f})} \approx \frac{\Delta\Gamma_d}{\Delta m_d} \tan \phi_d^{12}, \quad (1)$$

and is expressed in terms of the difference between the masses (Δm_d) and widths ($\Delta\Gamma_d$) of the mass eigenstates, and the CP -violating phase ϕ_d^{12} [5]. The Standard Model (SM) prediction, $a_{\text{sl}}^d = (-4.1 \pm 0.6) \times 10^{-4}$ [6], is small compared to experimental sensitivities. However, a_{sl}^d may be enhanced by virtual contributions from particles that exist in extensions to the SM [7].

The current most precise measurements are $a_{\text{sl}}^d = (0.06 \pm 0.17_{-0.32}^{+0.38})\%$ by the BaBar collaboration [8] and $a_{\text{sl}}^d = (0.68 \pm 0.45 \pm 0.14)\%$ by the D0 collaboration [9], where the first uncertainties are statistical and the second systematic. The D0 dimuon asymmetry, which is related to a linear combination of the semileptonic asymmetries in the B^0 and B_s^0 systems, disagrees with the theoretical predictions by 3.6 standard deviations. The LHCb collaboration has previously measured the semileptonic CP asymmetry in the B_s^0 system, a_{sl}^s [10], consistent with the SM. Improved experimental constraints are also required on a_{sl}^d to confirm or falsify the D0 anomaly.

In this analysis, a_{sl}^d is measured using semileptonic $B^0 \rightarrow D^- \mu^+ \nu_\mu X$ and $B^0 \rightarrow D^{*-} \mu^+ \nu_\mu X$ decays, where X denotes any additional particles due to possible feed-down from τ^+ decays into $\mu^+ X$ and higher-resonance D decays into $D^{(*)-} X$. The inclusion of charge-conjugate processes is implied. The signal is reconstructed from $D^{(*)-} \mu^+$ pairs, with the charm mesons reconstructed from $D^- \rightarrow K^+ \pi^- \pi^-$ and $D^{*-} \rightarrow \bar{D}^0 (\rightarrow K^+ \pi^-) \pi^-$ decays. A measurement of a_{sl}^d using the quantities in Eq. (1) requires determining (tagging) the flavour of the B^0 meson at production. Since this is inefficient in hadron collisions, a_{sl}^d is instead determined from the untagged decay rates. The number of observed final states as a function of the B^0 decay time is expressed as

$$N(t) \propto e^{-\Gamma_d t} \left[1 + \zeta A_D + \zeta \frac{a_{\text{sl}}^d}{2} - \zeta \left(A_P + \frac{a_{\text{sl}}^d}{2} \right) \cos \Delta m_d t \right], \quad (2)$$

where Γ_d is the B^0 decay width, and $\zeta = +1(-1)$ for the f (\bar{f}) final state. The asymmetry due to differences in detection efficiencies, ε , between f and \bar{f} final states,

$A_D \equiv [\varepsilon(f) - \varepsilon(\bar{f})]/[\varepsilon(f) + \varepsilon(\bar{f})]$, is determined using control samples of data, as described later. The asymmetry in the \bar{B}^0 and B^0 effective production cross sections, $A_P \equiv [\sigma(\bar{B}^0) - \sigma(B^0)]/[\sigma(\bar{B}^0) + \sigma(B^0)]$, and a_{sl}^d are determined simultaneously in a fit to the time-dependent rate of Eq. (2). Effects from higher-order asymmetry terms and a non-zero $\Delta\Gamma_d$, taken from experimental bounds [11], result in biases of less than 10^{-4} on a_{sl}^d and are ignored. The amount of direct CP violation in the Cabibbo-favoured decays $D^- \rightarrow K^+\pi^-\pi^-$ and $\bar{D}^0 \rightarrow K^+\pi^-$ is assumed to be negligible. The observed decay time of the semileptonic signal candidates is corrected using simulation since the final state is only partially reconstructed.

The LHCb detector [12] includes a high-precision tracking system with a dipole magnet, providing a measurement of momentum (p) and impact parameter (IP) for charged particles. The IP, defined as the minimum distance of a track to a proton–proton (pp) interaction vertex, is measured with a precision of about $20\ \mu\text{m}$ for high-momentum tracks. The polarity of the magnetic field is regularly reversed during data taking. Particle identification (PID) is provided by ring-imaging Cherenkov detectors, a calorimeter and a muon system. The trigger [13] consists of a hardware stage, based on information from the calorimeter and muon systems, followed by a software stage, which applies a full event reconstruction.

In the simulation, pp collisions are generated [14], and the interactions of the outgoing particles with the detector are modelled [15]. The B mesons are required to decay semileptonically to a muon, a neutrino and a $D^{(*)-}$ meson. Feed-down from higher D resonances and τ decays is based on branching fractions, either measured [11] or estimated assuming isospin symmetry.

The data used in this analysis correspond to a luminosity of $3.0\ \text{fb}^{-1}$, of which 1.0 (2.0) fb^{-1} was taken in 2011 (2012) at a pp centre-of-mass energy of 7 (8) TeV. The selection of candidates relies on the signatures of high-momentum tracks and displaced vertices from the B^0 , D^- and \bar{D}^0 decays. Candidate events are first required to pass the hardware trigger, which selects muons with momentum transverse to the beam direction (p_T) larger than 1.64 (1.76) GeV/c for the 2011 (2012) data. In a first stage of the software trigger, the muon is required to have a large IP. In a second stage, the muon and at least one of the $D^{(*)-}$ decay products are required to be consistent with the topological signature of b -hadron decays [13].

To suppress background, it is required that the tracks from the B^0 candidates do not point back to any pp interaction vertex. The muon, kaon and pion candidates are required to be well identified by the PID system. Tracks from the D^- , \bar{D}^0 and B^0 candidates are required to form well-defined vertices. For the $D^{*-}\mu^+$ final state, the difference between the D^{*-} and \bar{D}^0 masses should be between 144 and 147 MeV/c^2 . The mass of the $D^{(*)-}\mu^+$ final state is required to be between 3.0 and 5.2 GeV/c^2 to allow for missing particles in the final state; the upper limit removes background from four-body b -hadron decays. Misreconstructed D candidates made from random combinations of tracks are suppressed by requiring that the D^- or \bar{D}^0 decay time is larger than 0.1 ps. The contribution from charm decays directly produced in the pp interaction (prompt D) is reduced to below 0.1% by requiring D^- and \bar{D}^0 candidates to have an IP larger than $50\ \mu\text{m}$.

Detection asymmetries caused by left-right asymmetries in the reconstruction efficiency

change sign when the polarity of the LHCb magnet is inverted. Other asymmetries, such as those induced by differing nuclear cross sections for K^+ and K^- mesons, do not depend on the magnet polarity. The detection asymmetry of the $K^+\pi^-\pi^-\mu^+$ final state is factorized into a $\pi^-\mu^+$ component, where the pion is the hard one (i.e., from the \bar{D}^0 decay or the higher- p_T pion in the D^- decay), and a $K^+\pi^-$ component, where the pion is the soft one.

For the $\pi^-\mu^+$ component, any asymmetry arising from the different tracking efficiencies is suppressed by weighting the signal candidates such that the muon and hard pion have the same p_T and pseudorapidity (η) distributions. This reduces the effective sample size by about 40%, but makes the pion and muon appear almost symmetric to the tracking system. The asymmetry from the pion PID requirements is measured using a sample of unbiased $D^{*-} \rightarrow \bar{D}^0(\rightarrow K^+\pi^-)\pi^-$ decays, weighted to match the p_T and η distributions of the hard pions in the signal decays. The asymmetry from the muon PID and trigger requirements is measured using a low-background sample of $J/\psi \rightarrow \mu^+\mu^-$ decays with both muons reconstructed in the tracking system and with at least one muon without trigger and muon identification requirements. The J/ψ candidates are weighted such that the muons have the same p_T and η distributions as those in the signal decays.

For the $K^+\pi^-$ component, the detection asymmetry is determined using prompt D^- decays into $K^+\pi^-\pi^-$ and $K^0(\rightarrow \pi^+\pi^-)\pi^-$ final states [16]. This method assumes no direct CP violation in these two decay modes. The candidates in the calibration samples have the same PID requirements as those in the signal samples. The calibration samples are weighted such that the kinematic distributions of the particles agree with those of the kaon and soft pion in the signal samples. A small correction is applied to account for the K^0 detection and CP asymmetry [16]. The average $K^+\pi^-$ detection asymmetry is dominated by the difference in the nuclear interaction cross sections of K^+ and K^- mesons of approximately 1%.

The values of a_{sl}^d and A_P are determined from a two-dimensional maximum likelihood fit to the binned distributions of B^0 decay time and charm meson mass, simultaneously for both f and \bar{f} final states. The fit model consists of components for signal, background from B^+ decays to the same final state, and combinatorial background in the D mass distributions. The B^+ background comes from semileptonic B^+ decays into $D^{(*)-}\mu^+\nu_\mu$ and at least one other charged particle. As this background is difficult to distinguish from B^0 signal decays, fractions of this fit component are obtained from simulation and fixed in the fit to $(12.7 \pm 2.2)\%$ for the $D^-\mu^+$ sample and $(8.8 \pm 2.2)\%$ for the $D^{*-}\mu^+$ sample. The uncertainties are dominated by the knowledge of the branching fractions.

The mass distributions for D^- and D^0 candidates are shown in Fig. 1. To describe the mass distributions, the signal and B^+ background are modelled by a sum of two Gaussian functions with a power-law tail, and the combinatorial background by an exponential function.

To describe the time distributions, the signal is modelled by the decay rates of Eq. (2). The B^0 decay time is estimated from the B^0 flight distance L , the $D^{(*)-}\mu^+$ momentum p and the known B^0 mass m_B [11] as $t = \langle k \rangle m_B L / p$, where $\langle k \rangle$ represents a statistical correction accounting for the momentum of the missing particles in the final state. The value of $\langle k \rangle$ is determined from simulation as the average ratio between the reconstructed

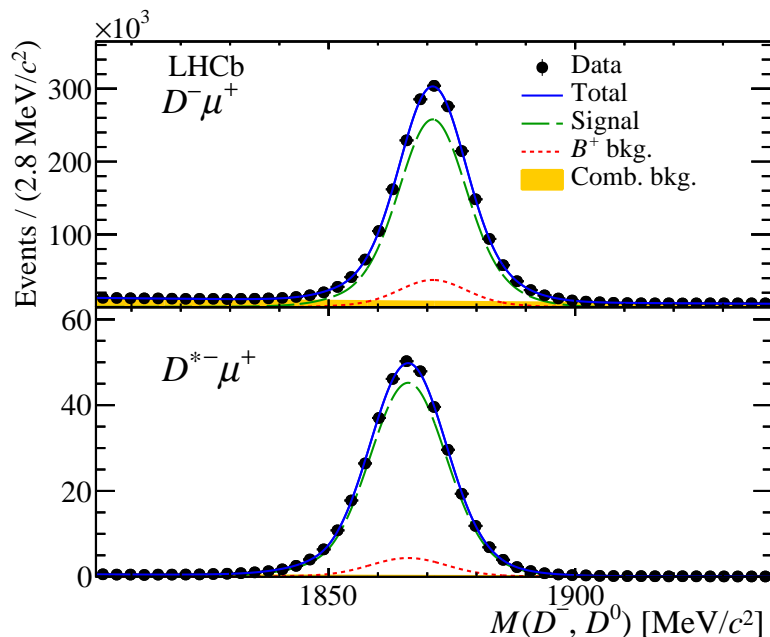


Figure 1: Mass distributions after weighting of (top) D^- candidates in the $D^- \mu^+$ sample and of (bottom) D^{*-} candidates in the $D^{*-} \mu^+$ sample, with fit results overlaid.

and true momenta of the B^0 meson, $k \equiv p_{\text{rec}}/p_{\text{true}}$. The value of $\langle k \rangle$ depends on the $D^{(*)-} \mu^+$ mass and is empirically parameterised by a second-order polynomial. This parameterisation is used to correct the B^0 decay time. After this mass correction, the $k/\langle k \rangle$ distribution has an RMS of 0.14. The decay time distribution in the fit is described as a convolution of the decay rates with the $k/\langle k \rangle$ distribution.

The efficiency as a function of the estimated decay time varies due to the IP requirements and track reconstruction effects. This is accounted for by multiplying the convoluted decay rates with an empirical acceptance function of the form $(1 - e^{-(t-t_0)/\alpha})(1 - \beta t)$, where t_0 and α describe the effect of the IP requirements, and β describes the track reconstruction effect. Since β is fully correlated with the B^0 lifetime, the latter is fixed to the known value [11], while β is allowed to vary in the fit.

The decay-time model for the B^+ background is similar to that of the signal, except that B^+ mesons do not mix. As the momentum spectra of the B^0 and B^+ decay products are nearly identical, the detection asymmetry is the same as that of the signal. The B^+ production asymmetry is taken as $(-0.6 \pm 0.6)\%$ from the observed asymmetry in $B^+ \rightarrow J/\psi K^+$ decays [17] after correcting for the kaon detection and measured CP asymmetries [11].

The combinatorial background in the D meson mass is dominated by other decays of charm hadrons produced in b -hadron decays. Hence, the decay-time model is the same as for the signal, but setting a_{sl}^d to zero. The corresponding values for A_P and A_D are allowed to vary in the fit.

In summary, the parameters related to the B^+ background, the detection asymmetry, Δm_d , Γ_d , t_0 , and the power-law tail in the mass distributions are fixed in the fit; all other parameters are allowed to vary. The fit is done in the decay-time interval $[1, 15]$ ps. The effective B^0 signal yield after weighting is 1.8 million in the $D^-\mu^+$ sample and 0.33 million in the $D^{*-\mu^+}$ sample.

Separate fits are done for the two magnet polarities, the 2011 and 2012 data-taking periods, and for the $D^-\mu^+$ and $D^{*-\mu^+}$ samples. To reduce the bias from any possible, unaccounted detection asymmetry, the arithmetic average of the measured values for the two magnet polarities is taken. The resulting a_{sl}^d values for the 2011 and 2012 run periods are combined with a weighted average. This gives $a_{\text{sl}}^d = (-0.19 \pm 0.21)\%$ for the $D^-\mu^+$ sample and $a_{\text{sl}}^d = (0.77 \pm 0.45)\%$ for the $D^{*-\mu^+}$ sample, where the uncertainties are only statistical. The production asymmetries are not averaged between the run periods as they may depend on the pp centre-of-mass energy. The decay rates and charge asymmetries as functions of the corrected decay time are shown in Fig. 2. The weighted averages from the $D^-\mu^+$ and $D^{*-\mu^+}$ samples are used to determine the final results. The separate fits give compatible results for a_{sl}^d and A_{P} . The largest difference is seen in the 2011 data for opposite magnet polarities, where a_{sl}^d differs by about two standard deviations. This is present in both decay modes and may arise from a statistical fluctuation of the detection asymmetry, which is highly correlated between the two decay samples. This difference is not seen in the larger 2012 data set.

The systematic uncertainties are listed in Table 1. The largest contribution comes from the detection asymmetry, where the dominant uncertainty is due to the limited size of the calibration samples. Additional uncertainties are assigned to account for background in the calibration samples, and the corresponding weighting procedures. The systematic effect from any residual tracking asymmetry is estimated using $J/\psi \rightarrow \mu^+\mu^-$ decays [18]. The uncertainty from a possible pion nuclear-interaction charge asymmetry is estimated to be 0.035%, using a parameterisation [11] of the measured cross sections of pions on deuterium [19], and the LHCb detector simulation.

The second largest contribution to the systematic uncertainty comes from the knowledge of the B^+ background, and is dominated by the B^+ production asymmetry. Uncertainties arising from the B^+ fraction, decay-time model, and acceptance are also taken into account. Other b -hadron backgrounds are expected from semileptonic Λ_b^0 and B_s^0 decays and from hadronic B decays. The fraction of background from $\Lambda_b^0 \rightarrow D^{(*)+}\mu^-\bar{\nu}_\mu X_n$ decays, where X_n represents any neutral baryonic state, is estimated to be roughly 2% using the ratio of Λ_b^0 to B^0 production cross sections [20], simulated efficiencies, and the branching ratio of $\Lambda_b^0 \rightarrow D^0 p \pi^-$ relative to that of $\Lambda_b^0 \rightarrow \Lambda_c^+ \pi^-$ decays [21]. The Λ_b^0 production asymmetry is estimated to be $(-0.9 \pm 1.5)\%$, determined from the raw asymmetry observed in $\Lambda_b^0 \rightarrow J/\psi p K^-$ [22] and subtracting kaon and proton detection asymmetries. The uncertainty on the Λ_b^0 production asymmetry results in a systematic uncertainty on a_{sl}^d of 0.07%. The systematic effect from an estimated 2% contribution from B_s^0 decays is small, since the production asymmetry vanishes due to the fast B_s^0 oscillations. Hadronic decays $B \rightarrow D^{(*)-}DX$, where the D meson decays semileptonically to produce a muon, have a different k -factor distribution compared to the signal. Simulation shows

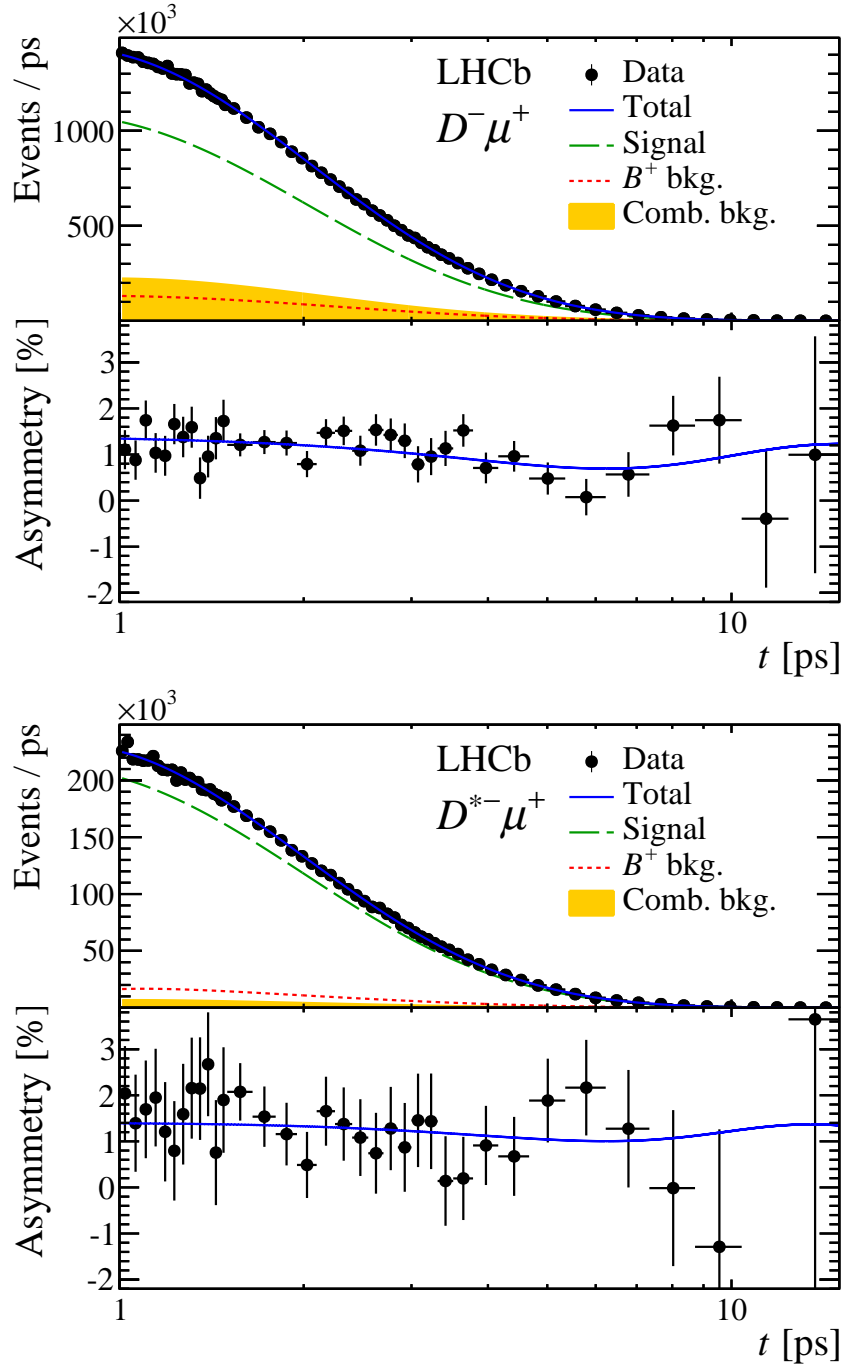


Figure 2: Decay rate and charge asymmetry after weighting versus decay time for (top) the $D^- \mu^+$ sample and (bottom) the $D^{*-} \mu^+$ sample. The data from the two run periods and magnet polarities are combined and the fit results are overlaid. The number of bins in the asymmetry plots is reduced for clarity. The visible asymmetry in these plots can be fully attributed to the non-zero detection and production asymmetries (not to a_{sl}^d), as explained in the text.

Table 1: Systematic uncertainties (in %) on a_{sl}^d and A_{P} for 7 and 8 TeV pp centre-of-mass energies. Entries marked with – are found to be negligible.

Source of uncertainty	a_{sl}^d	$A_{\text{P}}(7 \text{ TeV})$	$A_{\text{P}}(8 \text{ TeV})$
Detection asymmetry	0.26	0.20	0.14
B^+ background	0.13	0.06	0.06
A_b^0 background	0.07	0.03	0.03
B_s^0 background	0.03	0.01	0.01
Combinatorial D background	0.03	–	–
k -factor distribution	0.03	0.01	0.01
Decay-time acceptance	0.03	0.07	0.07
Knowledge of Δm_d	0.02	0.01	0.01
Quadratic sum	0.30	0.22	0.17

that these decays correspond to approximately 1% of the data and their effect is negligible. The systematic effect from the combinatorial background in the D mass distributions is assessed by varying the mass model in the fit.

The uncertainty on the shape of the k -factor distributions comes from uncertainties in the semileptonic branching fractions of B^0 mesons to higher-mass D resonances. Such decays are considered as signal, but have slightly different k -factor distributions. In the $D^- \mu^+$ sample about half of the D^- candidates originate from higher-mass D resonances. The uncertainties on these fractions are about 2%. The systematic effect on a_{sl}^d and A_{P} is determined by varying the fractions by 10% to account for possible unknown intermediate states. The effect of a dependence of the k -factor with B^0 decay time is small, and the effect on the difference in the B momentum distributions between data and simulation, evaluated using $B^+ \rightarrow J/\psi K^+$ decays, is negligible.

Systematic effects due to imperfect modelling of the decay time are tested by varying the acceptance function and extending the fit region down to 0.4 ps. The effect from varying Δm_d within its uncertainty [11] is taken into account. Effects associated with variations in B^0 decay-time binning are negligible.

The \bar{B}^0 – B^0 production asymmetries for the two centre-of-mass energies are $A_{\text{P}}(7 \text{ TeV}) = (-0.66 \pm 0.26 \pm 0.22)\%$ and $A_{\text{P}}(8 \text{ TeV}) = (-0.48 \pm 0.15 \pm 0.17)\%$, where the first uncertainty is statistical and the second systematic. These asymmetries refer to B^0 mesons in the ranges $2 < p_{\text{T}} < 30 \text{ GeV}/c$ and $2.0 < \eta < 4.8$, without correcting for p_{T} - and η -dependent reconstruction efficiencies. The production asymmetry at 7 TeV is compatible with previous results [23] and with the production asymmetry at 8 TeV. The determination of the CP asymmetry in semileptonic B^0 decays is

$$a_{\text{sl}}^d = (-0.02 \pm 0.19 \pm 0.30)\% ,$$

which is the most precise measurement to date and compatible with the SM prediction and earlier measurements [24].

Acknowledgements

We express our gratitude to our colleagues in the CERN accelerator departments for the excellent performance of the LHC. We thank the technical and administrative staff at the LHCb institutes. We acknowledge support from CERN and from the national agencies: CAPES, CNPq, FAPERJ and FINEP (Brazil); NSFC (China); CNRS/IN2P3 (France); BMBF, DFG, HGF and MPG (Germany); SFI (Ireland); INFN (Italy); FOM and NWO (The Netherlands); MNiSW and NCN (Poland); MEN/IFA (Romania); MinES and FANO (Russia); MinECo (Spain); SNSF and SER (Switzerland); NASU (Ukraine); STFC (United Kingdom); NSF (USA). The Tier1 computing centres are supported by IN2P3 (France), KIT and BMBF (Germany), INFN (Italy), NWO and SURF (The Netherlands), PIC (Spain), GridPP (United Kingdom). We are indebted to the communities behind the multiple open source software packages on which we depend. We are also thankful for the computing resources and the access to software R&D tools provided by Yandex LLC (Russia). Individual groups or members have received support from EPLANET, Marie Skłodowska-Curie Actions and ERC (European Union), Conseil général de Haute-Savoie, Labex ENIGMASS and OCEVU, Région Auvergne (France), RFBR (Russia), XuntaGal and GENCAT (Spain), Royal Society and Royal Commission for the Exhibition of 1851 (United Kingdom).

References

- [1] D0 collaboration, V. M. Abazov *et al.*, *Study of CP-violating charge asymmetries of single muons and like-sign dimuons in $p\bar{p}$ collisions*, Phys. Rev. **D89** (2014) 012002, [arXiv:1310.0447](#).
- [2] B. A. Dobrescu, P. J. Fox, and A. Martin, *CP violation in B_s mixing from heavy Higgs exchange*, Phys. Rev. Lett. **105** (2010) 041801, [arXiv:1005.4238](#).
- [3] S. Descotes-Genon and J. F. Kamenik, *A possible explanation of the D0 like-sign dimuon charge asymmetry*, Phys. Rev. **D87** (2013) 074036, [arXiv:1207.4483](#).
- [4] S. Sahoo, M. Kumar, and D. Banerjee, *The effect of Z' boson on same-sign dimuon charge asymmetry in $B_q^0 - \bar{B}_q^0$ system*, Int. J. Mod. Phys. **A28** (2013) 1350060, [arXiv:1306.5087](#).
- [5] A. Lenz and U. Nierste, *Theoretical update of $B_s - \bar{B}_s$ mixing*, JHEP **06** (2007) 072, [arXiv:hep-ph/0612167](#).
- [6] A. Lenz and U. Nierste, *Numerical updates of lifetimes and mixing parameters of B mesons*, [arXiv:1102.4274](#).
- [7] A. Lenz *et al.*, *Constraints on new physics in $B - \bar{B}$ mixing in the light of recent LHCb data*, Phys. Rev. **D86** (2012) 033008, [arXiv:1203.0238](#).

- [8] BaBar collaboration, J. P. Lees *et al.*, *Search for CP violation in B^0 - \bar{B}^0 mixing using partial reconstruction of $B^0 \rightarrow D^{*-} X \ell^+ \nu_\ell$ and a kaon tag*, Phys. Rev. Lett. **111** (2013) 101802, arXiv:1305.1575.
- [9] D0 collaboration, V. M. Abazov *et al.*, *Measurement of the semileptonic charge asymmetry in B^0 meson mixing with the D0 detector*, Phys. Rev. **D86** (2012) 072009, arXiv:1208.5813.
- [10] LHCb collaboration, R. Aaij *et al.*, *Measurement of the flavour-specific CP-violating asymmetry a_{sl}^s in B_s^0 decays*, Phys. Lett. **B728** (2014) 607, arXiv:1308.1048.
- [11] Particle Data Group, K. A. Olive *et al.*, *Review of particle physics*, Chin. Phys. **C38** (2014) 090001.
- [12] LHCb collaboration, A. A. Alves Jr. *et al.*, *The LHCb detector at the LHC*, JINST **3** (2008) S08005.
- [13] R. Aaij *et al.*, *The LHCb trigger and its performance in 2011*, JINST **8** (2013) P04022, arXiv:1211.3055.
- [14] T. Sjöstrand, S. Mrenna, and P. Skands, *PYTHIA 6.4 physics and manual*, JHEP **05** (2006) 026, arXiv:hep-ph/0603175; T. Sjöstrand, S. Mrenna, and P. Skands, *A brief introduction to PYTHIA 8.1*, Comput. Phys. Commun. **178** (2008) 852, arXiv:0710.3820; I. Belyaev *et al.*, *Handling of the generation of primary events in GAUSS, the LHCb simulation framework*, Nuclear Science Symposium Conference Record (NSS/MIC) **IEEE** (2010) 1155; D. J. Lange, *The EvtGen particle decay simulation package*, Nucl. Instrum. Meth. **A462** (2001) 152; P. Golonka and Z. Was, *PHOTOS Monte Carlo: a precision tool for QED corrections in Z and W decays*, Eur. Phys. J. **C45** (2006) 97, arXiv:hep-ph/0506026.
- [15] Geant4 collaboration, J. Allison *et al.*, *Geant4 developments and applications*, IEEE Trans. Nucl. Sci. **53** (2006) 270; Geant4 collaboration, S. Agostinelli *et al.*, *Geant4: a simulation toolkit*, Nucl. Instrum. Meth. **A506** (2003) 250; M. Clemencic *et al.*, *The LHCb simulation application, GAUSS: design, evolution and experience*, J. Phys. Conf. Ser. **331** (2011) 032023.
- [16] LHCb collaboration, R. Aaij *et al.*, *Measurement of CP asymmetry in $D^0 \rightarrow K^- K^+$ and $D^0 \rightarrow \pi^- \pi^+$ decays*, JHEP **07** (2014) 041, arXiv:1405.2797.
- [17] LHCb collaboration, R. Aaij *et al.*, *Measurement of CP asymmetries in the decays $B^0 \rightarrow K^{*0} \mu^+ \mu^-$ and $B^+ \rightarrow K^+ \mu^+ \mu^-$* , JHEP **09** (2014) 177, arXiv:1408.0978.
- [18] LHCb collaboration, R. Aaij *et al.*, *Measurement of the track reconstruction efficiency at LHCb*, arXiv:1408.1251, submitted to JINST.

- [19] W. Galbraith *et al.*, *Total cross sections of protons, anti-protons, and π and K mesons on hydrogen and deuterium in the momentum range 6-22 GeV/c*, Phys. Rev. **138** (1965) B913; A. S. Carroll *et al.*, *Total cross sections of π^\pm and K^\pm on protons and deuterons between 50 and 200 GeV/c*, Phys. Rev. Lett. **33** (1974) 932; A. S. Carroll *et al.*, *Total cross sections of π^\pm , K^\pm , p , and \bar{p} on protons and deuterons between 23 and 280 GeV/c*, Phys. Lett. **B61** (1976) 303; A. S. Carroll *et al.*, *Total cross sections of π^\pm , K^\pm , p and \bar{p} on protons and deuterons between 200 and 370 GeV/c*, Phys. Lett. **B80** (1979) 423.
- [20] LHCb collaboration, R. Aaij *et al.*, *Measurement of b hadron production fractions in 7 TeV pp collisions*, Phys. Rev. **D85** (2012) 032008, [arXiv:1111.2357](https://arxiv.org/abs/1111.2357).
- [21] LHCb collaboration, R. Aaij *et al.*, *Study of beauty baryon decays to $D^0 p h^-$ and $\Lambda_c^+ h^-$ final states*, Phys. Rev. **D89** (2014) 032001, [arXiv:1311.4823](https://arxiv.org/abs/1311.4823).
- [22] LHCb collaboration, R. Aaij *et al.*, *Observation of the $\Lambda_b^0 \rightarrow J/\psi p \pi^-$ decay*, JHEP **07** (2014) 103, [arXiv:1406.0755](https://arxiv.org/abs/1406.0755).
- [23] LHCb collaboration, R. Aaij *et al.*, *Measurement of the $\bar{B}^0 - B^0$ and $\bar{B}_s^0 - B_s^0$ production asymmetries in pp collisions at $\sqrt{s} = 7$ TeV*, Phys. Lett. **B739** (2014) 218, [arXiv:1408.0275](https://arxiv.org/abs/1408.0275).
- [24] Heavy Flavor Averaging Group, Y. Amhis *et al.*, *Averages of b -hadron, c -hadron, and τ -lepton properties as of early 2012*, [arXiv:1207.1158](https://arxiv.org/abs/1207.1158), updated results and plots available at <http://www.slac.stanford.edu/xorg/hfag/>.

LHCb collaboration

R. Aaij⁴¹, B. Adeva³⁷, M. Adinolfi⁴⁶, A. Affolder⁵², Z. Ajaltouni⁵, S. Akar⁶, J. Albrecht⁹, F. Alessio³⁸, M. Alexander⁵¹, S. Ali⁴¹, G. Alkhazov³⁰, P. Alvarez Cartelle³⁷, A.A. Alves Jr^{25,38}, S. Amato², S. Amerio²², Y. Amhis⁷, L. An³, L. Anderlini^{17,g}, J. Anderson⁴⁰, R. Andreassen⁵⁷, M. Andreotti^{16,f}, J.E. Andrews⁵⁸, R.B. Appleby⁵⁴, O. Aquines Gutierrez¹⁰, F. Archilli³⁸, A. Artamonov³⁵, M. Artuso⁵⁹, E. Aslanides⁶, G. Auriemma^{25,n}, M. Baalouch⁵, S. Bachmann¹¹, J.J. Back⁴⁸, A. Badalov³⁶, C. Baesso⁶⁰, W. Baldini¹⁶, R.J. Barlow⁵⁴, C. Barschel³⁸, S. Barsuk⁷, W. Barter⁴⁷, V. Batozskaya²⁸, V. Battista³⁹, A. Bay³⁹, L. Beaucourt⁴, J. Beddow⁵¹, F. Bedeschi²³, I. Bediaga¹, S. Belogurov³¹, K. Belous³⁵, I. Belyaev³¹, E. Ben-Haim⁸, G. Bencivenni¹⁸, S. Benson³⁸, J. Benton⁴⁶, A. Berezhnoy³², R. Bernet⁴⁰, M.-O. Bettler⁴⁷, M. van Beuzekom⁴¹, A. Bien¹¹, S. Bifani⁴⁵, T. Bird⁵⁴, A. Bizzeti^{17,i}, P.M. Bjørnstad⁵⁴, T. Blake⁴⁸, F. Blanc³⁹, J. Blouw¹⁰, S. Blusk⁵⁹, V. Bocci²⁵, A. Bondar³⁴, N. Bondar^{30,38}, W. Bonivento^{15,38}, S. Borghi⁵⁴, A. Borgia⁵⁹, M. Borsato⁷, T.J.V. Bowcock⁵², E. Bowen⁴⁰, C. Bozzi¹⁶, T. Brambach⁹, D. Brett⁵⁴, M. Britsch¹⁰, T. Britton⁵⁹, J. Brodzicka⁵⁴, N.H. Brook⁴⁶, H. Brown⁵², A. Bursche⁴⁰, J. Buytaert³⁸, S. Cadeddu¹⁵, R. Calabrese^{16,f}, M. Calvi^{20,k}, M. Calvo Gomez^{36,p}, P. Campana¹⁸, D. Campora Perez³⁸, A. Carbone^{14,d}, G. Carboni^{24,l}, R. Cardinale^{19,38,j}, A. Cardini¹⁵, L. Carson⁵⁰, K. Carvalho Akiba², G. Casse⁵², L. Cassina²⁰, L. Castillo Garcia³⁸, M. Cattaneo³⁸, Ch. Cauet⁹, R. Cenci²³, M. Charles⁸, Ph. Charpentier³⁸, M. Chefdeville⁴, S. Chen⁵⁴, S.-F. Cheung⁵⁵, N. Chiapolini⁴⁰, M. Chrzaszcz^{40,26}, X. Cid Vidal³⁸, G. Ciezarek⁴¹, P.E.L. Clarke⁵⁰, M. Clemencic³⁸, H.V. Cliff⁴⁷, J. Closier³⁸, V. Coco³⁸, J. Cogan⁶, E. Cogneras⁵, V. Cogoni¹⁵, L. Cojocariu²⁹, G. Collazuol²², P. Collins³⁸, A. Comerma-Montells¹¹, A. Contu^{15,38}, A. Cook⁴⁶, M. Coombes⁴⁶, S. Coquereau⁸, G. Corti³⁸, M. Corvo^{16,f}, I. Counts⁵⁶, B. Couturier³⁸, G.A. Cowan⁵⁰, D.C. Craik⁴⁸, M. Cruz Torres⁶⁰, S. Cunliffe⁵³, R. Currie⁵³, C. D'Ambrosio³⁸, J. Dalseno⁴⁶, P. David⁸, P.N.Y. David⁴¹, A. Davis⁵⁷, K. De Bruyn⁴¹, S. De Capua⁵⁴, M. De Cian¹¹, J.M. De Miranda¹, L. De Paula², W. De Silva⁵⁷, P. De Simone¹⁸, C.-T. Dean⁵¹, D. Decamp⁴, M. Deckenhoff⁹, L. Del Buono⁸, N. Déleage⁴, D. Derkach⁵⁵, O. Deschamps⁵, F. Dettori³⁸, A. Di Canto³⁸, H. Dijkstra³⁸, S. Donleavy⁵², F. Dordei¹¹, M. Dorigo³⁹, A. Dosil Suárez³⁷, D. Dossett⁴⁸, A. Dovbnya⁴³, K. Dreimanis⁵², G. Dujany⁵⁴, F. Dupertuis³⁹, P. Durante³⁸, R. Dzhelyadin³⁵, A. Dziurda²⁶, A. Dzyuba³⁰, S. Easo^{49,38}, U. Egede⁵³, V. Egorychev³¹, S. Eidelman³⁴, S. Eisenhardt⁵⁰, U. Eitschberger⁹, R. Ekelhof⁹, L. Eklund⁵¹, I. El Rifai⁵, Ch. Elsasser⁴⁰, S. Ely⁵⁹, S. Esen¹¹, H.-M. Evans⁴⁷, T. Evans⁵⁵, A. Falabella¹⁴, C. Färber¹¹, C. Farinelli⁴¹, N. Farley⁴⁵, S. Farry⁵², R.F. Fay⁵², D. Ferguson⁵⁰, V. Fernandez Albor³⁷, F. Ferreira Rodrigues¹, M. Ferro-Luzzi³⁸, S. Filippov³³, M. Fiore^{16,f}, M. Fiorini^{16,f}, M. Firlej²⁷, C. Fitzpatrick³⁹, T. Fiutowski²⁷, P. Fol⁵³, M. Fontana¹⁰, F. Fontanelli^{19,j}, R. Forty³⁸, O. Francisco², M. Frank³⁸, C. Frei³⁸, M. Frosini^{17,g}, J. Fu^{21,38}, E. Furfaro^{24,l}, A. Gallas Torreira³⁷, D. Galli^{14,d}, S. Gallorini^{22,38}, S. Gambetta^{19,j}, M. Gandelman², P. Gandini⁵⁹, Y. Gao³, J. García Pardiñas³⁷, J. Garofoli⁵⁹, J. Garra Tico⁴⁷, L. Garrido³⁶, D. Gascon³⁶, C. Gaspar³⁸, R. Gauld⁵⁵, L. Gavardi⁹, A. Geraci^{21,v}, E. Gersabeck¹¹, M. Gersabeck⁵⁴, T. Gershon⁴⁸, Ph. Ghez⁴, A. Gianelle²², S. Gianì³⁹, V. Gibson⁴⁷, L. Giubega²⁹, V.V. Gligorov³⁸, C. Göbel⁶⁰, D. Golubkov³¹, A. Golutvin^{53,31,38}, A. Gomes^{1,a}, C. Gotti²⁰, M. Grabalosa Gándara⁵, R. Graciani Diaz³⁶, L.A. Granado Cardoso³⁸, E. Graugés³⁶, E. Graverini⁴⁰, G. Graziani¹⁷, A. Grecu²⁹, E. Greening⁵⁵, S. Gregson⁴⁷, P. Griffith⁴⁵, L. Grillo¹¹, O. Grünberg⁶³, B. Gui⁵⁹, E. Gushchin³³, Yu. Guz^{35,38}, T. Gys³⁸, C. Hadjivasiliou⁵⁹, G. Haefeli³⁹, C. Haen³⁸, S.C. Haines⁴⁷, S. Hall⁵³, B. Hamilton⁵⁸, T. Hampson⁴⁶, X. Han¹¹, S. Hansmann-Menzemer¹¹, N. Harnew⁵⁵, S.T. Harnew⁴⁶, J. Harrison⁵⁴, J. He³⁸, T. Head³⁸,

V. Heijne⁴¹, K. Hennessy⁵², P. Henrard⁵, L. Henry⁸, J.A. Hernando Morata³⁷,
 E. van Herwijnen³⁸, M. Heß⁶³, A. Hicheur², D. Hill⁵⁵, M. Hoballah⁵, C. Hombach⁵⁴,
 W. Hulsbergen⁴¹, P. Hunt⁵⁵, N. Hussain⁵⁵, D. Hutchcroft⁵², D. Hynds⁵¹, M. Idzik²⁷, P. Ilten⁵⁶,
 R. Jacobsson³⁸, A. Jaeger¹¹, J. Jalocha⁵⁵, E. Jans⁴¹, P. Jatou³⁹, A. Jawahery⁵⁸, F. Jing³,
 M. John⁵⁵, D. Johnson³⁸, C.R. Jones⁴⁷, C. Joram³⁸, B. Jost³⁸, N. Jurik⁵⁹, S. Kandybei⁴³,
 W. Kanso⁶, M. Karacson³⁸, T.M. Karbach³⁸, S. Karodia⁵¹, M. Kelsey⁵⁹, I.R. Kenyon⁴⁵,
 T. Ketel⁴², B. Khanji^{20,38}, C. Khurewathanakul³⁹, S. Klaver⁵⁴, K. Klimaszewski²⁸,
 O. Kochebina⁷, M. Kolpin¹¹, I. Komarov³⁹, R.F. Koopman⁴², P. Koppenburg^{41,38}, M. Korolev³²,
 A. Kozlinskiy⁴¹, L. Kravchuk³³, K. Kreplin¹¹, M. Kreps⁴⁸, G. Krocker¹¹, P. Krokovny³⁴,
 F. Kruse⁹, W. Kucewicz^{26,o}, M. Kucharczyk^{20,26,k}, V. Kudryavtsev³⁴, K. Kurek²⁸,
 T. Kvaratskheliya³¹, V.N. La Thi³⁹, D. Lacarrere³⁸, G. Lafferty⁵⁴, A. Lai¹⁵, D. Lambert⁵⁰,
 R.W. Lambert⁴², G. Lanfranchi¹⁸, C. Langenbruch⁴⁸, B. Langhans³⁸, T. Latham⁴⁸,
 C. Lazzeroni⁴⁵, R. Le Gac⁶, J. van Leerdam⁴¹, J.-P. Lees⁴, R. Lefèvre⁵, A. Leflat³²,
 J. Lefrançois⁷, S. Leo²³, O. Leroy⁶, T. Lesiak²⁶, B. Leverington¹¹, Y. Li³, T. Likhomanenko⁶⁴,
 M. Liles⁵², R. Lindner³⁸, C. Linn³⁸, F. Lionetto⁴⁰, B. Liu¹⁵, S. Lohn³⁸, I. Longstaff⁵¹,
 J.H. Lopes², N. Lopez-March³⁹, P. Lowdon⁴⁰, D. Lucchesi^{22,r}, H. Luo⁵⁰, A. Lupato²²,
 E. Luppi^{16,f}, O. Lupton⁵⁵, F. Machefert⁷, I.V. Machikhiliyan³¹, F. Maciuc²⁹, O. Maev³⁰,
 S. Malde⁵⁵, A. Malinin⁶⁴, G. Manca^{15,e}, G. Mancinelli⁶, A. Mapelli³⁸, J. Maratas⁵,
 J.F. Marchand⁴, U. Marconi¹⁴, C. Marin Benito³⁶, P. Marino^{23,t}, R. Märki³⁹, J. Marks¹¹,
 G. Martellotti²⁵, A. Martín Sánchez⁷, M. Martinelli³⁹, D. Martinez Santos^{42,38},
 F. Martinez Vidal⁶⁵, D. Martins Tostes², A. Massafferri¹, R. Matev³⁸, Z. Mathe³⁸,
 C. Matteuzzi²⁰, B. Maurin³⁹, A. Mazurov⁴⁵, M. McCann⁵³, J. McCarthy⁴⁵, A. McNab⁵⁴,
 R. McNulty¹², B. McSkelly⁵², B. Meadows⁵⁷, F. Meier⁹, M. Meissner¹¹, M. Merk⁴¹,
 D.A. Milanes⁶², M.-N. Minard⁴, N. Moggi¹⁴, J. Molina Rodriguez⁶⁰, S. Monteil⁵, M. Morandin²²,
 P. Morawski²⁷, A. Mordà⁶, M.J. Morello^{23,t}, J. Moron²⁷, A.-B. Morris⁵⁰, R. Mountain⁵⁹,
 F. Muheim⁵⁰, K. Müller⁴⁰, M. Mussini¹⁴, B. Muster³⁹, P. Naik⁴⁶, T. Nakada³⁹,
 R. Nandakumar⁴⁹, I. Nasteva², M. Needham⁵⁰, N. Neri²¹, S. Neubert³⁸, N. Neufeld³⁸,
 M. Neuner¹¹, A.D. Nguyen³⁹, T.D. Nguyen³⁹, C. Nguyen-Mau^{39,q}, M. Nicol⁷, V. Niess⁵,
 R. Niet⁹, N. Nikitin³², T. Nikodem¹¹, A. Novoselov³⁵, D.P. O'Hanlon⁴⁸,
 A. Oblakowska-Mucha^{27,38}, V. Obraztsov³⁵, S. Oggero⁴¹, S. Ogilvy⁵¹, O. Okhrimenko⁴⁴,
 R. Oldeman^{15,e}, C.J.G. Onderwater⁶⁶, M. Orlandea²⁹, J.M. Otalora Goicochea², A. Otto³⁸,
 P. Owen⁵³, A. Oyanguren⁶⁵, B.K. Pal⁵⁹, A. Palano^{13,c}, F. Palombo^{21,u}, M. Palutan¹⁸,
 J. Panman³⁸, A. Papanestis^{49,38}, M. Pappagallo⁵¹, L.L. Pappalardo^{16,f}, C. Parkes⁵⁴,
 C.J. Parkinson^{9,45}, G. Passaleva¹⁷, G.D. Patel⁵², M. Patel⁵³, C. Patrignani^{19,j}, A. Pearce⁵⁴,
 A. Pellegrino⁴¹, M. Pepe Altarelli³⁸, S. Perazzini^{14,d}, P. Perret⁵, M. Perrin-Terrin⁶,
 L. Pescatore⁴⁵, E. Pesen⁶⁷, K. Petridis⁵³, A. Petrolini^{19,j}, E. Picatoste Olloqui³⁶, B. Pietrzyk⁴,
 T. Pilar⁴⁸, D. Pinci²⁵, A. Pistone¹⁹, S. Playfer⁵⁰, M. Plo Casasus³⁷, F. Polci⁸, A. Poluektov^{48,34},
 E. Polcarpo², A. Popov³⁵, D. Popov¹⁰, B. Popovici²⁹, C. Potterat², E. Price⁴⁶, J.D. Price⁵²,
 J. Prisciandaro³⁹, A. Pritchard⁵², C. Prouve⁴⁶, V. Pugatch⁴⁴, A. Puig Navarro³⁹, G. Punzi^{23,s},
 W. Qian⁴, B. Rachwal²⁶, J.H. Rademacker⁴⁶, B. Rakotomiamanana³⁹, M. Rama¹⁸,
 M.S. Rangel², I. Raniuk⁴³, N. Rauschmayr³⁸, G. Raven⁴², F. Redi⁵³, S. Reichert⁵⁴, M.M. Reid⁴⁸,
 A.C. dos Reis¹, S. Ricciardi⁴⁹, S. Richards⁴⁶, M. Rihl³⁸, K. Rinnert⁵², V. Rives Molina³⁶,
 P. Robbe⁷, A.B. Rodrigues¹, E. Rodrigues⁵⁴, P. Rodriguez Perez⁵⁴, S. Roiser³⁸,
 V. Romanovsky³⁵, A. Romero Vidal³⁷, M. Rotondo²², J. Rouvinet³⁹, T. Ruf³⁸, H. Ruiz³⁶,
 P. Ruiz Valls⁶⁵, J.J. Saborido Silva³⁷, N. Sagidova³⁰, P. Sail⁵¹, B. Saitta^{15,e},
 V. Salustino Guimaraes², C. Sanchez Mayordomo⁶⁵, B. Sanmartin Sedes³⁷, R. Santacesaria²⁵,

C. Santamarina Rios³⁷, E. Santovetti^{24,l}, A. Sarti^{18,m}, C. Satriano^{25,n}, A. Satta²⁴,
D.M. Saunders⁴⁶, D. Savrina^{31,32}, M. Schiller⁴², H. Schindler³⁸, M. Schlupp⁹, M. Schmelling¹⁰,
B. Schmidt³⁸, O. Schneider³⁹, A. Schopper³⁸, M. Schubiger³⁹, M.-H. Schune⁷, R. Schwemmer³⁸,
B. Sciascia¹⁸, A. Sciubba²⁵, A. Semennikov³¹, I. Sepp⁵³, N. Serra⁴⁰, J. Serrano⁶, L. Sestini²²,
P. Seyfert¹¹, M. Shapkin³⁵, I. Shapoval^{16,43,f}, Y. Shcheglov³⁰, T. Shears⁵², L. Shekhtman³⁴,
V. Shevchenko⁶⁴, A. Shires⁹, R. Silva Coutinho⁴⁸, G. Simi²², M. Sirendi⁴⁷, N. Skidmore⁴⁶,
I. Skillicorn⁵¹, T. Skwarnicki⁵⁹, N.A. Smith⁵², E. Smith^{55,49}, E. Smith⁵³, J. Smith⁴⁷, M. Smith⁵⁴,
H. Snoek⁴¹, M.D. Sokoloff⁵⁷, F.J.P. Soler⁵¹, F. Soomro³⁹, D. Souza⁴⁶, B. Souza De Paula²,
B. Spaan⁹, P. Spradlin⁵¹, S. Sridharan³⁸, F. Stagni³⁸, M. Stahl¹¹, S. Stahl¹¹, O. Steinkamp⁴⁰,
O. Stenyakin³⁵, S. Stevenson⁵⁵, S. Stoica²⁹, S. Stone⁵⁹, B. Storaci⁴⁰, S. Stracka²³,
M. Straticiuc²⁹, U. Straumann⁴⁰, R. Stroili²², V.K. Subbiah³⁸, L. Sun⁵⁷, W. Sutcliffe⁵³,
K. Swientek²⁷, S. Swientek⁹, V. Syropoulos⁴², M. Szczekowski²⁸, P. Szczypka^{39,38}, T. Szumlak²⁷,
S. T'Jampens⁴, M. Teklishyn⁷, G. Tellarini^{16,f}, F. Teubert³⁸, C. Thomas⁵⁵, E. Thomas³⁸,
J. van Tilburg⁴¹, V. Tisserand⁴, M. Tobin³⁹, J. Todd⁵⁷, S. Tolk⁴², L. Tomassetti^{16,f},
D. Tonelli³⁸, S. Topp-Joergensen⁵⁵, N. Torr⁵⁵, E. Tournefier⁴, S. Tourneur³⁹, M.T. Tran³⁹,
M. Tresch⁴⁰, A. Trisovic³⁸, A. Tsaregorodtsev⁶, P. Tsopelas⁴¹, N. Tuning⁴¹, M. Ubeda Garcia³⁸,
A. Ukleja²⁸, A. Ustyuzhanin⁶⁴, U. Uwer¹¹, C. Vacca¹⁵, V. Vagnoni¹⁴, G. Valenti¹⁴, A. Vallier⁷,
R. Vazquez Gomez¹⁸, P. Vazquez Regueiro³⁷, C. Vázquez Sierra³⁷, S. Vecchi¹⁶, J.J. Velthuis⁴⁶,
M. Veltri^{17,h}, G. Veneziano³⁹, M. Vesterinen¹¹, B. Viaud⁷, D. Vieira², M. Vieites Diaz³⁷,
X. Vilasis-Cardona^{36,p}, A. Vollhardt⁴⁰, D. Volyanskyy¹⁰, D. Voong⁴⁶, A. Vorobyev³⁰,
V. Vorobyev³⁴, C. Voß⁶³, J.A. de Vries⁴¹, R. Waldi⁶³, C. Wallace⁴⁸, R. Wallace¹², J. Walsh²³,
S. Wandernoth¹¹, J. Wang⁵⁹, D.R. Ward⁴⁷, N.K. Watson⁴⁵, D. Websdale⁵³, M. Whitehead⁴⁸,
J. Wicht³⁸, D. Wiedner¹¹, G. Wilkinson^{55,38}, M. Wilkinson⁵⁹, M.P. Williams⁴⁵, M. Williams⁵⁶,
H.W. Wilschut⁶⁶, F.F. Wilson⁴⁹, J. Wimberley⁵⁸, J. Wishahi⁹, W. Wislicki²⁸, M. Witek²⁶,
G. Wormser⁷, S.A. Wotton⁴⁷, S. Wright⁴⁷, K. Wyllie³⁸, Y. Xie⁶¹, Z. Xing⁵⁹, Z. Xu³⁹, Z. Yang³,
X. Yuan³, O. Yushchenko³⁵, M. Zangoli¹⁴, M. Zavertyaev^{10,b}, L. Zhang⁵⁹, W.C. Zhang¹²,
Y. Zhang³, A. Zhelezov¹¹, A. Zhokhov³¹, L. Zhong³.

¹ Centro Brasileiro de Pesquisas Físicas (CBPF), Rio de Janeiro, Brazil

² Universidade Federal do Rio de Janeiro (UFRJ), Rio de Janeiro, Brazil

³ Center for High Energy Physics, Tsinghua University, Beijing, China

⁴ LAPP, Université de Savoie, CNRS/IN2P3, Annecy-Le-Vieux, France

⁵ Clermont Université, Université Blaise Pascal, CNRS/IN2P3, LPC, Clermont-Ferrand, France

⁶ CPPM, Aix-Marseille Université, CNRS/IN2P3, Marseille, France

⁷ LAL, Université Paris-Sud, CNRS/IN2P3, Orsay, France

⁸ LPNHE, Université Pierre et Marie Curie, Université Paris Diderot, CNRS/IN2P3, Paris, France

⁹ Fakultät Physik, Technische Universität Dortmund, Dortmund, Germany

¹⁰ Max-Planck-Institut für Kernphysik (MPIK), Heidelberg, Germany

¹¹ Physikalisches Institut, Ruprecht-Karls-Universität Heidelberg, Heidelberg, Germany

¹² School of Physics, University College Dublin, Dublin, Ireland

¹³ Sezione INFN di Bari, Bari, Italy

¹⁴ Sezione INFN di Bologna, Bologna, Italy

¹⁵ Sezione INFN di Cagliari, Cagliari, Italy

¹⁶ Sezione INFN di Ferrara, Ferrara, Italy

¹⁷ Sezione INFN di Firenze, Firenze, Italy

¹⁸ Laboratori Nazionali dell'INFN di Frascati, Frascati, Italy

¹⁹ Sezione INFN di Genova, Genova, Italy

²⁰ Sezione INFN di Milano Bicocca, Milano, Italy

²¹ Sezione INFN di Milano, Milano, Italy

- ²² *Sezione INFN di Padova, Padova, Italy*
- ²³ *Sezione INFN di Pisa, Pisa, Italy*
- ²⁴ *Sezione INFN di Roma Tor Vergata, Roma, Italy*
- ²⁵ *Sezione INFN di Roma La Sapienza, Roma, Italy*
- ²⁶ *Henryk Niewodniczanski Institute of Nuclear Physics Polish Academy of Sciences, Kraków, Poland*
- ²⁷ *AGH - University of Science and Technology, Faculty of Physics and Applied Computer Science, Kraków, Poland*
- ²⁸ *National Center for Nuclear Research (NCBJ), Warsaw, Poland*
- ²⁹ *Horia Hulubei National Institute of Physics and Nuclear Engineering, Bucharest-Magurele, Romania*
- ³⁰ *Petersburg Nuclear Physics Institute (PNPI), Gatchina, Russia*
- ³¹ *Institute of Theoretical and Experimental Physics (ITEP), Moscow, Russia*
- ³² *Institute of Nuclear Physics, Moscow State University (SINP MSU), Moscow, Russia*
- ³³ *Institute for Nuclear Research of the Russian Academy of Sciences (INR RAN), Moscow, Russia*
- ³⁴ *Budker Institute of Nuclear Physics (SB RAS) and Novosibirsk State University, Novosibirsk, Russia*
- ³⁵ *Institute for High Energy Physics (IHEP), Protvino, Russia*
- ³⁶ *Universitat de Barcelona, Barcelona, Spain*
- ³⁷ *Universidad de Santiago de Compostela, Santiago de Compostela, Spain*
- ³⁸ *European Organization for Nuclear Research (CERN), Geneva, Switzerland*
- ³⁹ *Ecole Polytechnique Fédérale de Lausanne (EPFL), Lausanne, Switzerland*
- ⁴⁰ *Physik-Institut, Universität Zürich, Zürich, Switzerland*
- ⁴¹ *Nikhef National Institute for Subatomic Physics, Amsterdam, The Netherlands*
- ⁴² *Nikhef National Institute for Subatomic Physics and VU University Amsterdam, Amsterdam, The Netherlands*
- ⁴³ *NSC Kharkiv Institute of Physics and Technology (NSC KIPT), Kharkiv, Ukraine*
- ⁴⁴ *Institute for Nuclear Research of the National Academy of Sciences (KINR), Kyiv, Ukraine*
- ⁴⁵ *University of Birmingham, Birmingham, United Kingdom*
- ⁴⁶ *H.H. Wills Physics Laboratory, University of Bristol, Bristol, United Kingdom*
- ⁴⁷ *Cavendish Laboratory, University of Cambridge, Cambridge, United Kingdom*
- ⁴⁸ *Department of Physics, University of Warwick, Coventry, United Kingdom*
- ⁴⁹ *STFC Rutherford Appleton Laboratory, Didcot, United Kingdom*
- ⁵⁰ *School of Physics and Astronomy, University of Edinburgh, Edinburgh, United Kingdom*
- ⁵¹ *School of Physics and Astronomy, University of Glasgow, Glasgow, United Kingdom*
- ⁵² *Oliver Lodge Laboratory, University of Liverpool, Liverpool, United Kingdom*
- ⁵³ *Imperial College London, London, United Kingdom*
- ⁵⁴ *School of Physics and Astronomy, University of Manchester, Manchester, United Kingdom*
- ⁵⁵ *Department of Physics, University of Oxford, Oxford, United Kingdom*
- ⁵⁶ *Massachusetts Institute of Technology, Cambridge, MA, United States*
- ⁵⁷ *University of Cincinnati, Cincinnati, OH, United States*
- ⁵⁸ *University of Maryland, College Park, MD, United States*
- ⁵⁹ *Syracuse University, Syracuse, NY, United States*
- ⁶⁰ *Pontifícia Universidade Católica do Rio de Janeiro (PUC-Rio), Rio de Janeiro, Brazil, associated to ²*
- ⁶¹ *Institute of Particle Physics, Central China Normal University, Wuhan, Hubei, China, associated to ³*
- ⁶² *Departamento de Física, Universidad Nacional de Colombia, Bogota, Colombia, associated to ⁸*
- ⁶³ *Institut für Physik, Universität Rostock, Rostock, Germany, associated to ¹¹*
- ⁶⁴ *National Research Centre Kurchatov Institute, Moscow, Russia, associated to ³¹*
- ⁶⁵ *Instituto de Física Corpuscular (IFIC), Universitat de Valencia-CSIC, Valencia, Spain, associated to ³⁶*
- ⁶⁶ *Van Swinderen Institute, University of Groningen, Groningen, The Netherlands, associated to ⁴¹*
- ⁶⁷ *Celal Bayar University, Manisa, Turkey, associated to ³⁸*

^a *Universidade Federal do Triângulo Mineiro (UFMT), Uberaba-MG, Brazil*

^b *P.N. Lebedev Physical Institute, Russian Academy of Science (LPI RAS), Moscow, Russia*

^c *Università di Bari, Bari, Italy*

- ^d *Università di Bologna, Bologna, Italy*
- ^e *Università di Cagliari, Cagliari, Italy*
- ^f *Università di Ferrara, Ferrara, Italy*
- ^g *Università di Firenze, Firenze, Italy*
- ^h *Università di Urbino, Urbino, Italy*
- ⁱ *Università di Modena e Reggio Emilia, Modena, Italy*
- ^j *Università di Genova, Genova, Italy*
- ^k *Università di Milano Bicocca, Milano, Italy*
- ^l *Università di Roma Tor Vergata, Roma, Italy*
- ^m *Università di Roma La Sapienza, Roma, Italy*
- ⁿ *Università della Basilicata, Potenza, Italy*
- ^o *AGH - University of Science and Technology, Faculty of Computer Science, Electronics and Telecommunications, Kraków, Poland*
- ^p *LIFAELS, La Salle, Universitat Ramon Llull, Barcelona, Spain*
- ^q *Hanoi University of Science, Hanoi, Viet Nam*
- ^r *Università di Padova, Padova, Italy*
- ^s *Università di Pisa, Pisa, Italy*
- ^t *Scuola Normale Superiore, Pisa, Italy*
- ^u *Università degli Studi di Milano, Milano, Italy*
- ^v *Politecnico di Milano, Milano, Italy*